tvst

Article

Color Fundus Autofluorescence to Determine Activity of Macular Neovascularization in Age-Related Macular Degeneration

Stela Vujosevic[1,2], Caterina Toma[2], Valentina Sarao[3,4], Daniele Veritti[3], Marco Brambilla[5], Andrea Muraca[2], Stefano De Cillà[2,6], Edoardo Villani[1,7], Paolo Nucci[7], and Paolo Lanzetta[3,4]

[1] Eye Clinic IRCCS MultiMedica, Milan, Italy
[2] University Hospital Maggiore della Carità, Eye Clinic, Novara, Italy
[3] Department of Medicine-Ophthalmology, University of Udine, Udine, Italy
[4] Istituto Europeo di Microchirurgia Oculare-IEMO, Udine, Italy
[5] Department of Medical Physics, University Hospital Maggiore Della Carità, Novara, Italy
[6] Department of Health Sciences, University East Piedmont "A. Avogadro," Novara, Italy
[7] Department of Clinical Sciences and Community Health, University of Milan, Milan, Italy

Correspondence: Stela Vujosevic, Eye Clinic IRCCS MultiMedica, Via San Vittore 12, 20123 Milan, Italy. e-mail: stela.vujosevic@gmail.com; stela.vujosevic@unimi.it

Received: July 22, 2020
Accepted: January 10, 2021
Published: February 22, 2021

Keywords: color fundus autofluorescence; age-related macular degeneration; macular neovascularization; disease activity; fluorophores

Citation: Vujosevic S, Toma C, Sarao V, Veritti D, Brambilla M, Muraca A, De Cillà S, Villani E, Nucci P, Lanzetta P. Color fundus autofluorescence to determine activity of macular neovascularization in age-related macular degeneration. Trans Vis Sci Tech. 2021;10(2):33, https://doi.org/10.1167/tvst.10.2.33

Purpose: To evaluate with color fundus autofluorescence (FAF) different lesion components of macular neovascularization (MNV) secondary to age-related macular degeneration (AMD) and to assess its activity.

Methods: In total, 137 eyes (102 patients) with MNV underwent a complete eye examination, including color fundus photography, optical coherence tomography (OCT), OCT angiography, and confocal color FAF, with an excitation wavelength at 450 nm. Each image was imported into a custom-image analysis software for quantitative estimation of emission wavelength and green and red emission fluorescence (GEFC/REFC) intensity, considering both single components of neovascular AMD and different MNV types (type 1 and type 2 MNV, active and inactive MNV).

Results: Subretinal fluid (SRF) had significantly higher values of GEFC ($P = 0.008$ and $P = 0.0004$) and REFC intensity ($P = 0.005$ and $P = 0.0003$) versus fibrosis and atrophy. The emission wavelength from SRF was lower compared to atrophy ($P = 0.024$) but not to fibrosis ($P = 0.46$). No significant differences were detected between type 1 and 2 MNV. Considering active versus inactive MNVs, a difference was detected for all evaluated parameters ($P < 0.001$). Mean FAF wavelength of both MNV with SRF and intraretinal fluid (IRF) was lower versus inactive MNV ($P < 0.001$ and $P = 0.005$). MNV with SRF ($P < 0.001$) had higher values of GEFC and REFC versus inactive MNV ($P < 0.001$). MNV with IRF had higher values of GEFC versus inactive MNV ($P = 0.05$).

Conclusions: Quantitative color FAF can differentiate active versus inactive MNV, whereas no differences were found between type 1 and type 2 MNV. If these data can be further confirmed, color FAF may be useful for automatic detection of active MNV in AMD and as a guide for treatment.

Translational Relevance: Automatic quantitative evaluation of green and red emission components of FAF in AMD can help determine the activity of MNV and guide the treatment.

Introduction

Neovascular age-related macular degeneration (nAMD) remains the most common cause of visual impairment in patients with age-related macular degeneration (AMD) despite the introduction of anti-vascular endothelial growth factor (VEGF) treatment.[1] Diagnosis of nAMD is made mostly by fundus examination and multimodal imaging, which led recently to a new terminology of nAMD, namely, macular neovascularization (MNV) secondary to AMD.[2]

Conventional fundus autofluorescence (FAF) (488 nm) and near-infrared autofluorescence have been used in nAMD for evaluation of the status of the retinal pigment epithelium (RPE) in MNV with fluid and also for the evaluation of new development or enlargement of preexisting atrophy during the treatment.[1,3–9] Moreover, FAF can be used as a prognostic parameter in nAMD, as a predominantly preserved FAF pattern in the macula showed better visual acuity (VA) outcome.[5] Using conventional confocal blue light at 488 nm, detected FAF is mostly due to the lipofuscin in the RPE. Lipofuscin is a by-product of phagocytosis of the photoreceptor outer segments and accumulates in the RPE with age, contributing to the pathogenesis of AMD.[10] Lipofuscin has a broad spectrum of excitation (300–600 nm) and emission (480–800 nm) wavelengths. There are more than 10 fluorophores identified so far that may be responsible for the FAF signal at different wavelengths. Besides lipofuscin, these include lipofuscin-like lipopigments, vitamin A (retinols and carotenoids), protoporphyrin IX and porphyrin derivates, fatty acids (accumulated lipids), flavins (coenzymes of key enzymes in redox reactions), nicotinamide adenine dinucleotide phosphate, collagen/elastin (extracellular fibrous proteins), cytokeratins (intracellular fibrous proteins), and aromatic amino acids (phenylalanine, tyrosine, and triptophane; functional proteins).[11] Thus, fluorescence of the ocular fundus may be related to various pathologic processes, including also the advanced glycation end products (AGEs), and may be regarded as a general feature of aging and disease progression.[12,13]

The possibility to discriminate different fluorophores and lesion components may help in the diagnosis and management of nAMD. Recently, a novel short-wavelength confocal blue autofluorescence system has been available, using a 450-nm excitation wavelength. This instrument has a possibility to obtain the so-called color FAF that uses two different emission spectral channels, the shorter component (green, at 510–560 nm) and the longer one (red, at 560–700 nm). In this way, there is a potential to isolate minor fluorophores that otherwise would be overwhelmed by the lipofuscin.[14] There are very limited data in the literature on the use of color FAF in geographic atrophy.[14,15] No data are currently available on the use of color FAF in nAMD, especially in the quantitative estimation of green and red emission spectra for assessing the activity of MNV.

The aim of this study was to quantitatively evaluate different lesion components in the context of MNV secondary to AMD to determine if color FAF can be useful to discern between active and inactive MNV and may be used noninvasively as adjunctive information when deciding treatment.

Materials and Methods

Patients and Study Design

In this prospective, observational, cross-sectional case evaluation, we consecutively enrolled 137 eyes (102 patients) affected by macular nAMD, both active and inactive, who presented at the Medical Retina Service of the Eye Clinic (University Hospital Maggiore della Carità, Novara, Italy) and at the Ambulatory Surgery Center Istituto Europeo di Microchirugia Oculare-IEMO, Udine, Italy, from September 1 to 30, 2019. Diagnosis and assessment of disease activity were based on clinical examination performed by expert retinal specialists (SV and VS) and confirmed by multimodal retinal imaging.

Inclusion criteria were diagnosis of unilateral or bilateral macular nAMD with and without signs of active disease, both treatment naive and previously treated with anti-VEGF, and pseudophakia or only mild cataract (not precluding good-quality imaging). Exclusion criteria were any maculopathy other than macular nAMD, previous vitreoretinal surgery, use of drugs that could interfere with macular function (e.g., hydroxychloroquine, tamoxifen), and poor quality of imaging due to significant media opacity or poor fixation. Active disease was defined as the presence of exudation at the time of clinical evaluation confirmed by detection of subretinal and/or intraretinal fluid on OCT.

Anamnestic data concerning disease history were carefully collected. Each patient underwent a complete eye examination, including best-corrected visual acuity (BCVA), determined at 4 m with standard Early Treatment Diabetic Retinopathy Study (ETDRS) charts, intraocular pressure measurement, dilated fundus examination with a 90-D lens, and noninvasive multimodal imaging with color fundus photography (CFP), swept-source OCT (SS-OCT) and OCT

angiography (OCT-A), and FAF. Fluorescein angiography was performed in case of first diagnosis of nAMD, as per usual clinical practice.

The study adhered to the tenets of the Declaration of Helsinki and was approved by the institutional Ethics Committee; each patient signed a written informed consent prior to image acquisition.

Imaging

SS-OCT

SS-OCT and SS-OCT-A scans were acquired using DRI SS-OCT/OCT-A Triton plus (Topcon Europe Medical BV, Capelle aan den IJssel, The Netherlands). The acquisition protocol included 9-mm radial and five line-cross OCT scans centered on the fovea, as well as a three-dimensional 4.5-mm × 4.5-mm OCT-A map of the macula. OCT and OCT-A images were used to define the diagnosis of type 1 and type 2 MNV according to the new classification proposed by Spaide et al.[2] Moreover, OCT B-scans were carefully examined to detect signs of MNV activity, defined as the presence of intraretinal and/or subretinal fluid (intraretinal cysts, serous or hemorrhagic detachment of the neuroretina)[16,17] and serous, hemorrhagic, or fibrovascular pigment epithelium detachment (PED). OCT-A en-face images were used to confirm the presence and topographic colocalization of MNV when evaluating FAF images.

Color Fundus Photography and Fundus Autofluorescence

CFPs and FAF images were acquired using a confocal light-emitting diode (LED) fundus imaging system (EIDON; CenterVue, Padua, Italy). The confocal LED blue-light FAF device has an excitation wavelength between 440 and 475 nm (peak at 450 nm) and emission detection between 500 and 750 nm. In this device, the full-emission spectrum is detected on a color sensor, providing so-called color FAF images, consisting of only the red (range 560–700 nm) and green (range 500–560 nm) emission fluorescence components (REFCs/GEFCs). The device is fully automated. With a single exposure, a 60-degree (horizontal) × 55-degree (vertical) image (resolution 3680 × 3288 pixels) of the posterior pole was acquired. Two different graders (CT and VS) carefully and independently reviewed all images to check for good quality prior to further analyses, since it could significantly influence the results. Moreover, they identified and localized each component present in the context of the macular lesion by comparing color FAF images with corresponding true color photos and OCT and OCT-A scans. Finally, the two graders compared the gradings, and in case of disagreement, one grader (SV) gave the final adjudication on the quality of images and identification of single-lesion components.

In particular, the following lesion components were considered: MNV, hemorrhage (He), subretinal fluid (SRF), intraretinal fluid (IRF), PED, fibrosis, and atrophy.

Color FAF Image Analysis

For each eye, the original color FAF image was exported and imported into the custom-made image analysis software "FAF Color Segmentation Tool" purposely designed by the manufacturer for the quantitative evaluation of these images, as previously described.[18] This software is able to separately and quantitatively measure the long-wavelength (red-R) and short-wavelength (green-G) components of the emission spectrum (emission fluorescence components, REFCs and GEFCs) of each pixel of the image. The software provides an estimation of the wavelength by means of an exponential model based on the proportion of GEFCs and REFCs. Fluorescence intensity and emission wavelengths of each pixel of the image are displayed in a two-dimensional *xy* graph (segment graph), where emission wavelength is reported on the x-axis and intensity on the y-axis. A second xy-graph (explore graph) quantifies the intensity of the REFC (x-axis) and of the GEFC (y-axis) for each pixel of the image.

Since the software is able to elaborate data of fluorescence for each pixel but not differentiate between different lesion components contributing to the final fluorescence of a specific pixel, only regions where the single component was clearly identifiable were considered in the final analysis. IRF with cystoid spaces was excluded from the analysis of single-lesion signal because it could not be clearly isolated from the other components. All the images were carefully evaluated for the presence of any artifacts (i.e., eye movement, iris blockage, etc.), and in such a case, they were manually excluded from the data set.

To achieve more reliable results for each lesion, data of fluorescence were recorded at four different sites (pixel squares, each corresponding to approximately 5 × 5 μm^2), and a mean of these four values was computed (Fig. 1). All images were rechecked by one author (SV) to ensure correct evaluation of single lesions.

After this first step, a second analysis was performed differentiating active from inactive MNV and type 1 from type 2 MNV, as previously described. Active MNV was further analyzed based on the presence of SRF or IRF colocalizing with the MNV. Eyes with hemorrhages masquerading the MNV were excluded

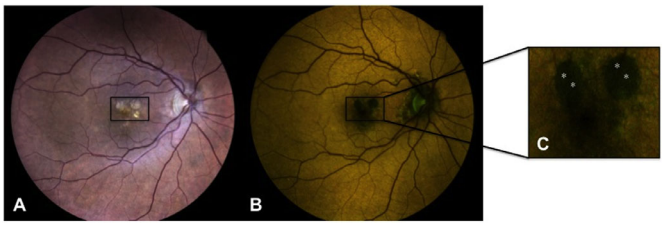

Figure 1. Example image showing the methodology used for analysis. (A) True-color fundus photography showing the presence of circular areas of chorioretinal atrophy (in the *black box*) in the context of neovascular AMD. (B) Corresponding color FAF image. (C) Detail of color FAF image showing the four analyzed sites (highlighted by *white asterisks*). The image analysis software recorded the following values for the four sites: site 1 wavelength 580.6, GEFC 22, REFC 24; site 2 wavelength 580.9, GEFC 21, REFC 25; site 3 wavelength 577.1, GEFC 24.5, REFC 24.5; site 4 wavelength 579.6, GEFC 21, REFC 20.5.

from this analysis. Data of fluorescence (fluorescence intensity and emission wavelength, intensity of the REFCs and GEFCs) were recorded at 10 different sites, and a mean of these 10 values was computed.

Statistical Analyses

The means of the experimental groups were reported as arithmetic mean (standard deviation) and median (range) for continuous variables in the text and tables. Differences in the means of the dependent variables (red-R, green-G, intensity, and emission wavelengths) were studied with analysis of variance (ANOVA) methods.

In the first analysis, a one-way ANOVA was used to assess the impact of the different types of lesions (SRF, fibrosis, and atrophy) on the dependent variables.

A two-way ANOVA with principal effects was employed in the second analysis. The first two-level factor was MNV type. The second three-level factor was the status (active or inactive) of MNV. Active MNVs were further evaluated based on the presence of SRF versus IRF. When a principal effect was found, a post hoc Scheffé test was used to identify the sources of variability.

Analysis was performed with Statistica version 6.0 (StatSoft, Tulsa, OK, USA) using a two-sided type I error rate of $P = 0.05$.

Results

Of 137 eyes (102 patients) initially recruited in the study, 97 eyes (80 patients) were included in the final analysis. Twenty-six eyes were excluded due to poor quality of FAF imaging (due to motion artifacts, iris blockage, or media opacities) and 14 eyes due to advanced nAMD (large disciform scars) with complete subversion of macular morphology with impossibility to identify single components of lesions.

Mean age was 79.5 ± 8.4 years (range, 50–96 years); 54 patients were women and 26 were men. All patients were of Caucasian ethnicity. Twenty-one eyes had treatment-naive nAMD (13 eyes with type 1 MNV, 8 eyes with type 2 MNV) and 76 eyes had previously treated nAMD (mean number of previous anti-VEGF injections was 8.6 ± 5.8); 57 eyes had active nAMD and 40 eyes inactive nAMD on clinical examination and OCT. Mean BCVA was 75.6 ± 16.8 ETDRS letters in eyes with active MNV and 59.1 ± 20.2 ETDRS letters in eyes with inactive MNV.

Mean values, median, and range of FAF wavelength and intensity of GEFCs and REFCs of different evaluated lesions (MNV, He, SRF, PED, fibrosis, atrophy) are reported in Table 1.

Compared to fibrosis and atrophy, SRF had significantly higher values of GEFC intensity ($P = 0.008$ and $P = 0.0004$) and REFC intensity ($P = 0.005$ and $P = 0.0003$). The emission wavelength from all the evaluated lesions was within the yellow wavelength spectrum. However, the emission wavelength from SRF was significantly lower compared to atrophy ($P = 0.024$) but not to fibrosis ($P = 0.46$). No significant differences were detected between fibrosis and atrophy for the analyzed parameters.

Mean values, median, and range of FAF wavelength and intensity of GEFCs and REFCs of the different evaluated MNV types (type 1 and type 2 MNV, MNV with IRF or SRF, inactive MNV) are reported in Table 2.

As for comparison between type 1 MNV and type 2 MNV, no significant differences were detected for the analyzed parameters ($P = 0.75$). Therefore, for subsequent analyses between active and inactive MNV, type 1 and type 2 MNV were considered together.

Considering all active MNVs together versus inactive MNV, a significant difference was detected for all evaluated parameters ($P < 0.001$). Mean FAF wavelength of both MNV with SRF and IRF was significantly lower than that of inactive MNV ($P < 0.001$ and $P = 0.005$, respectively). No significant differences were detected for mean FAF wavelength between MNV with SRF and IRF. MNV with SRF had significantly higher values of GEFC and REFC intensity compared to MNV with IRF ($P = 0.002$ and $P < 0.001$, respectively) and inactive MNV ($P < 0.001$). MNV with IRF had a higher mean value of GEFC versus inactive MNV ($P = 0.05$), and an increasing

Table 1. FAF Wavelength and GEFC and REFC Intensity of Different Lesion Components in Macular Neovascularization

Lesion	Wavelength	GEFC Intensity	REFC Intensity
MNV			
Mean ± SD	577.3 ± 4.66	57.24 ± 34.24	63.89 ±31.41
Median	577.43	43.13	57.75
Range	567.9–590.98	1–124	18–134
He			
Mean ± SD	584.72 ± 8.21	19.27 ± 18.86	26.6 ± 18.13
Median	585.45	12.38	12.38
Range	573.5–600	0–63	0–63
SRF			
Mean ± SD	576.92 ± 1.83	95.98 ± 64.66	105.49 ± 67.17
Median	577.06	69.75	112.0
Range	573.3–579.3	13.75–238.25	16.0–255.0
PED			
Mean ± SD	577.08 ± 3.71	63.29 ± 43.47	68.96 ± 41.24
Median	578.24	47.75	56.25
Range	572.35–584.55	15.5–182.25	19.25–180.0
Fibrosis			
Mean ± SD	580.2 ± 8.0	42.5 ± 41.2	49.8 ± 38.0
Median	577.38	37.5	41.5
Range	568.33–594.9	1–164	5–132.75
Atrophy			
Mean ± SD	585.2 ± 8.0	17.9 ± 18.7	26.6 ± 17.4
Median	574.08	29.5	28.75
Range	579.1–594.1	2–116.75	5–98.250

trend was detected for REFC intensity versus inactive MNV (Table 3 and Figs. 2–4).

Of 16 eyes with active MNV and IRF on OCT, 9 (56.25%) had signs of fibrosis, 3 (18.75%) had outer retina and RPE atrophy, and only 4 eyes (25%) had also SRF, in a different location of MNV and IRF. Eyes with active MNV and IRF had lower mean BCVA (66.43 ± 20.51 letters) versus eyes with active MNV and SRF (79.69 ± 13.43 letters), $P = 0.07$.

Discussion

In the present study, we report on quantitatively determined color FAF data in nAMD. Eyes with both active and inactive nAMD lesions (type 1 and 2 MNV), as determined by clinical evaluation, OCT, and OCT-A, were analyzed. Different single components, such as SRF, intra/subretinal He, PED, subretinal fibrosis, and atrophy, were separately evaluated.

The autofluorescence of the fundus is a complex phenomenon and depends on different fluorophores. The fluorescence from the lipofuscin and *N*-retinylidene-*N*-retinylethanolamine (A2E) is mostly responsible for the FAF intensity in the longer-wavelength emission range (mostly the red spectrum, between 580 and 700 nm). However, all other minor fluorophores contribute mostly to the FAF intensity in the shorter-wavelength emission range (green spectrum, above 500 nm to 560 nm). These minor fluorophores may be better excited at a shorter, blue wavelength.[14] These include, besides A2E, the oxidized fluorescent form flavin adenine dinucleotide (FAD) of the redox pair FAD–FADH2, important for evaluation of the metabolic state of the photoreceptor's inner-segment mitochondria (with single maximum-emission FAF at 524 nm); AGEs (the extracellular material, accumulating in older patients in soft drusen, basal laminar deposits, and RPE cells and considered biomarkers of aging)[19,20]; and, in limited amount, collagen 2 (emission at 508 nm), due to the reduced fluorescence intensity down to 20% at a 450-nm wavelength excitation.[9,21]

In the present study, all the considered lesion components had the overlapping spectrum of mean

Table 2. FAF Wavelength and GEFC and REFC Intensity of Different MNV Types

MNV Type	Wavelength	GEFC Intensity	REFC Intensity
MNV1 active + IRF (10)			
Mean ± SD	575.7 ± 4.45	59.08 ± 29.30	58.75 ± 27.40
Median	576.17	53.35	52
Range	566.34–581.03	12.1–97.3	15.8–107.5
MNV1 active + SRF (14)			
Mean ± SD	576.5 ± 3.0	88.89 ± 43.14	95.41 ± 40.43
Median	577.38	92.9	94.8
Range	571.61–581.18	24.2–150.7	26.2–148.3
MNV1 inactive (22)			
Mean ± SD	579.76 ± 5.99	31.54 ± 21.95	35.42 ± 21.53
Median	578.95	22.9	27.65
Range	571.69–593.55	8.2–77.7	10.8–89.7
MNV2 active + IRF (6)			
Mean ± SD	576.32 ± 1.83	56.15 ± 42.69	57.37 ± 36.64
Median	576.23	42.10	44.85
Range	573.57–579.18	16.3–129.7	21.9–118.8
MNV2 active + SRF (18)			
Mean ± SD	575.53 ± 2.22	104.97 ± 50.73	106.86 ± 48.41
Median	575.65	129.4	125.4
Range	570.34–578.87	40.3–182.2	41.6–170.4
MNV2 inactive (18)			
Mean ± SD	582.59 ± 7.33	32.29 ± 26.38	37.45 ± 24.66
Median	580.12	19.4	24.6
Range	569.99–596.1	4.4–86.9	9–86.8

Table 3. Comparison between Active and Inactive MNVs

MNV Type	Wavelength	GEFC Intensity	REFC Intensity
Active	575.9 ± 2.9	84.6 ± 47.0	87.3 ± 45.2
+ SRF	575.9 ± 2.6[a]	97.9 ± 47.5	101.8 ± 44.8
+ IRF	575.9 ± 3.6[b]	58.0 ± 33.5[c,d]	58.2 ± 30.0[e]
Inactive	581.0 ± 6.7	31.9 ± 23.7[e]	36.3 ± 22.7[e]
P value[f]	<0.001	<0.001	<0.001

[a]Comparison versus inactive MNVs: Scheffé's test, $P < 0.001$.

[b]Comparison versus inactive MNVs: Scheffé's test, $P = 0.005$.

[c]Comparison versus inactive MNVs: Scheffé's test, $P = 0.05$.

[d]Comparison versus active MNVs + SRF: Scheffé's test, $P = 0.002$.

[e]Comparison versus active MNVs + SRF: Scheffé's test, $P < 0.001$.

[f]Two-way ANOVA analyses: comparison between patients with active and inactive MNV. Statistical significance was set at $P = 0.05$. Values are reported as mean ± SD.

FAF emission in the range between 566 and 600 nm when excited by the short-wavelength blue light (at 450 nm). The only difference found was between atrophy and SRF, with SRF emitting at a shorter wavelength.

However, when evaluating quantitative data on FAF obtained automatically by the current software, one should bear in mind that the FAF value is the weighted average emission value of that wavelength (as stated by the manufacturer). Thus, it would mean that a specific FAF emission wavelength value may be due to a single emitted wavelength from the lesion or to two different wavelengths but with equal GEFC and REFC intensity. Therefore, this value needs to be integrated with clinical (morphologic/functional/metabolic) data of the patient to be more appropriately interpreted. For example, in the present study, SRF had much higher intensity in the REFCs versus GEFCs, whereas the mean FAF wavelength was 576.92 ± 1.83 nm, similar to other lesion components. Therefore, the red emission fluorophores (such as the lipofuscin and the A2E) contribute more than the fluorophores in the green wavelength spectrum within the SRF for the similar

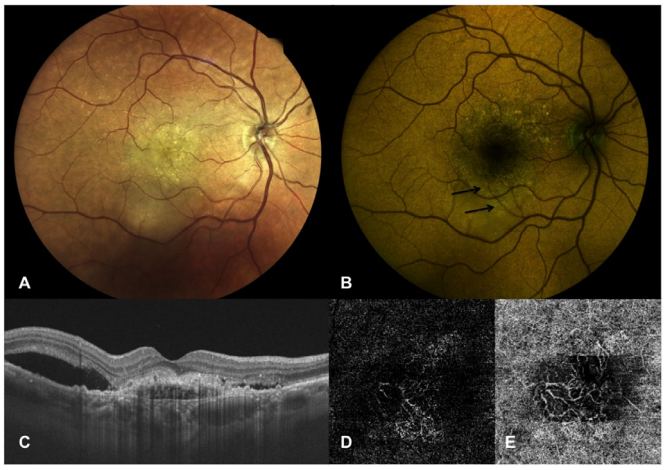

Figure 2. Right eye of a 78-year-old female patient with active MNV secondary to AMD. (A) True-color fundus photography showing a *yellowish* central area corresponding to MNV with subretinal fluid expanding in particular inferiorly to the fovea. (B) Color FAF showing a high intensity of the emitting components at the site of SRF (REFC intensity 80, GEFC intensity 69.75) at a mean wavelength of 576.96 nm (indicated by *black arrows*). (C) OCT vertical B-scan centered on the fovea showing a subfoveal active MNV as demonstrated by the presence of SRF adjacent to the MNV. (D, E) OCT-A slabs showing a neovascular net interesting both the outer retina (D) and choriocapillaris (E).

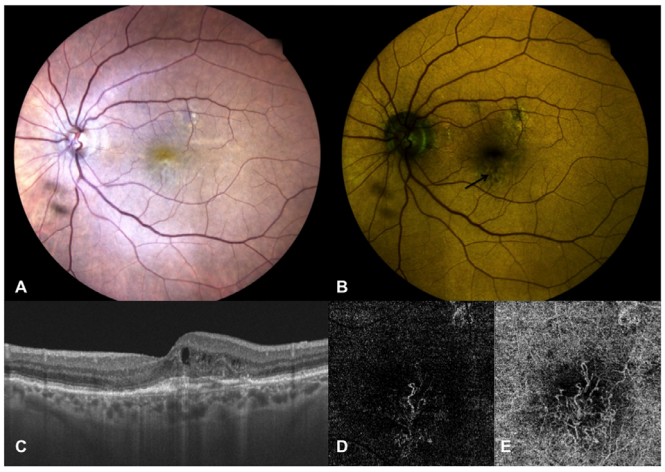

Figure 3. Left eye of an 85-year-old female patient affected by active MNV secondary to AMD. (A) True-color fundus photography showing a *whitish-yellowish* central area. (B) Color FAF showing irregular areas of altered autofluorescence surrounding the fovea (indicated by *black arrow*), with higher intensity of the quantitatively evaluated emitting components in *red* (REFC intensity 71.9, GEFC intensity 57.4) at a mean wavelength of 579.09 nm. (C) OCT vertical B-scan centered on the fovea showing thickened subfoveal outer retina layers with overlying small intraretinal cysts and initial outer retina tubulations; no SRF is detectable. (D, E) OCT-A of the outer retina (D) and choriocapillaris (E) slabs showing a neovascular net interesting both slabs but with larger size of the MNV detected at the choriocapillaris.

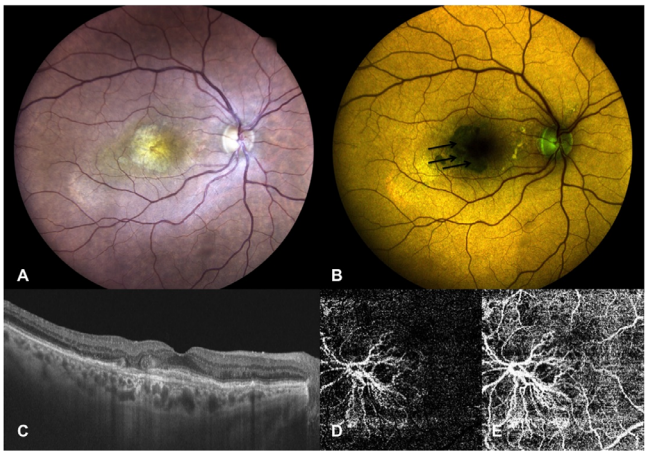

Figure 4. Right eye of a 77-year-old female patient affected by inactive MNV secondary to AMD. (A) True-color fundus photography showing presence of a fibrovascular lesion. (B) Color FAF showing reduced intensity of the quantitatively evaluated emitting autofluorescence components (REFC intensity 24.1, GEFC intensity 22.5) at a mean wavelength of 588.17 nm (indicated by *black arrows*). (C) OCT horizontal B-scan centered on the fovea showing thickened subfoveal outer retina layers with no signs of MNV activity (SRF or IRF) and perifoveal outer retina tubulations. (D, E) OCT-A of the outer retina (D) and choriocapillaris (E) slabs showing a large neovascular net interesting both slabs.

final FAF emission wavelength as for the other detected components in nAMD. Moreover, SRF had much higher fluorescence emission intensities than atrophy and subretinal fibrosis. The significance of this finding is that many more fluorophores are present/excited in SRF versus atrophy and fibrosis. In fact, the latter lesions are characterized by hypo-autofluorescence with conventional blue FAF (at 488 nm) due to the loss of the RPE cells and decrease in lipofuscin granules.[22] However, in the present study, some green and red emission fluorophores were still detected in both atrophy and subretinal fibrosis. Although the present data cannot be directly compared to other studies, due to different methodology of FAF evaluation, our data are in line with data documented by Borrelli et al.,[14] who evaluated the presence and pattern of GEFC signal in 25 eyes with atrophic AMD, applying a custom-made image-processing algorithm in which the REFC was subtracted and only the GEFC was evaluated within the areas of macular atrophy. The authors concluded that GEFC signal was due to the presence of hyperreflective material overlying Bruch's membrane (either residual sub-RPE deposits or regressing drusen).[14,23] In a different study on atrophic AMD (and no signs of present or past MNV), the authors also reported a high capability of this new FAF device to accurately detect the site and size of atrophic lesions (after the isolation of the REFC).[15]

More recently, the same group further validated the use of color FAF in a healthy population and confirmed that the quantitative evaluation of GEFC has high reliability and repeatability, suggesting its potential usefulness in assessing the retinal metabolic status in different diseases such as AMD and diabetes.[24]

The importance of discriminating different fluorophores may be useful for functional evaluation of metabolic alterations of the retina during AMD. Fundus structures that can produce the FAF include the RPE (with lipofuscin granules), Bruch's membrane, and the sub-RPE deposits (drusen).[22] Using a spectrophotometric detector with a scanning laser confocal microscope, Marmorstein et al.[22] documented that Bruch's membrane and sub-RPE deposits were excited by overlapping spectra in the blue light and ultraviolet light, and the emission fluorescence was detected in the blue-green range at higher intensities in human donor eyes with AMD than in age-matched control eyes. In fact, histologic data confirmed that Bruch's membrane is formed by five layers: RPE–basal lamina (BL), inner collagenous layer called the sub-RPE–basal lamina space, elastic layer, outer collagenous layer, and choriocapillaris-BL.[25] Therefore, certain contributions from the connective tissue (collagen/elastin) to the FAF in Bruch's membrane cannot be excluded.[19,25]

AGEs may play an important role in aging and neovascularization.[20] The progressive buildup of these compounds may alter the structure and function of proteins and may also contribute to the pathology of metabolic diseases, such as diabetes, atherosclerosis, and oxidative stress and inflammation associated with neurodegenerative diseases of aging.[19] AGEs stimulate VEGF expression in cultured and in vivo RPE cells, induce endothelial cells to secrete VEGF, and have an in vitro angiogenic effect; therefore, the accumulation of AGEs in soft drusen, basal laminar deposits, and RPE cells may lead to overexpression of VEGF, transforming growth factor-beta (TGFb), and platelet-derived growth factor (PDGF); development of nAMD; and fibrosis.[20,26–29]

When evaluating different types of MNV (type 1 and type 2), no differences in FAF parameters were observed. Significant differences were found when comparing active versus inactive MNV. Active MNVs were considered those with subretinal or intraretinal fluid on OCT, which is commonly used in clinical practice to guide treatment decisions, whereas the use of fluorescein angiography has decreased significantly.[16,17,30] The differences included lower mean FAF wavelengths and higher intensities of both green and red emission components in active versus inactive MNV. Especially active MNV with SRF had the highest values in both green and red emission spectra. When we separately evaluated active MNV with SRF versus MNV with IRF, we noticed that MNV with IRF had more signs of chronicity, including fibrosis and outer retina and RPE atrophy on OCT, and a trend to lower BCVA. This negative impact of IRF (cysts) on BCVA versus SRF was also reported in the Comparison of AMD Treatments Trials (CATT) trial, probably due to apoptotic and necrotic cell death, visible on OCT as small intraretinal cysts.[31] Therefore, the values of GEFCs and REFCs were lower than in MNV with SRF with less chronic disease. These quantitative data obtained with color FAF can be considered in line with data obtained with standard blue (488-nm) FAF in neovascular AMD. Whereas an increased pattern of FAF corresponded well with SRF and the edges of the choroidal neovascularization (CNV), indicating a significant accumulation of lipofuscin caused by the compensatory proliferation of RPE cells proximal to CNV when disease progresses,[32] and just in some cases with drusen, a decreased FAF pattern corresponded to fibrovascular/disciform scar, macular atrophy, blood, pigmentary RPE changes, and, in one-third of cases, active MNV.[4,33–36] McBain et al.[6] reported reduced FAF in 90% of eyes with classic CNV (above the RPE, type 2 MNV), whereas in occult CNV (beneath the RPE, type 1 MNV), areas of increased FAF were present, clinically corresponding to SRF. The origin of the increased FAF signal was explained as an increased content in RPE lipofuscin secondary to increased outer segment shedding at sites of chronic neurosensory retinal detachment.[37,38] The decreased FAF (488 nm) documented in classic CNV could not be distinguished from decreased FAF due to macular atrophy, whereas in color FAF, these lesions had very distinct parameters (Tables 1, 2). Moreover, color FAF allows one to separately detect fluorescence deriving also from minor fluorophores and, with the use of the specific software, to separately quantify the emission intensity in the green and red spectra. In this way, the activity of MNV can be discerned from nonactive MNV, thus supporting a decision on the need for treatment. As quantitative evaluation gives more precise data than qualitative evaluation of color FAF, this method may offer a possibility for automatic evaluation of the images with an indication for treatment. This would need to be confirmed in larger and possibly longitudinal studies.

Besides the intrinsic limits of this new imaging method (as previously described), the major limitations of this study include the lack of longitudinal data in order to evaluate correlation to visual acuity outcomes, as well as the inclusion of patients with pseudophakia or only with mild cataract. The 450-nm

FAF is influenced by the lens condition; therefore, its use in patients with more advanced cataracts and the quality of obtained data need to be further evaluated. However, the color FAF image is rather easily interpretable, as it is actually a standard colored picture that does not need any postprocessing in order to be analyzed.

In conclusion, to our knowledge, this is the first study to evaluate quantitative data obtained in automatic fashion on color FAF in nAMD, evaluating separately green and red emission components of the FAF. Significantly different data were documented for active versus inactive MNV, while no differences were found for type 1 versus type 2 MNV. If these data can be further confirmed and validated in larger studies comparing the color FAF to other imaging modalities (*in primis* OCT, etc.), color FAF, with an easy and fast single-shot image acquisition, may become a useful tool for the automatic detection of active MNV and for guiding the treatment.

Acknowledgments

Disclosure: **S. Vujosevic,** None; **C. Toma,** None; **V. Sarao,** None; **D. Veritti,** None; **M. Brambilla,** None; **A. Muraca,** None; **S. De Cillà,** None; **E. Villani,** None; **P. Nucci,** None; **P. Lanzetta,** None

References

1. Lois N, Forrester JV. *Fundus Autofluorescence*. 2nd ed. Philadelphia: Lippincott Williams & Wilkins; 2015.
2. Spaide RF, Jaffe GJ, Sarraf D, et al. Consensus nomenclature for reporting neovascular age-related macular degeneration data. *Ophthalmology.* 2020;127:616–636.
3. Lanzetta P, Cruess AF, Cohen SY, et al. Predictors of visual outcomes in patients with neovascular age-related macular degeneration treated with anti-vascular endothelial growth factor therapy: post hoc analysis of the VIEW studies. *Acta Ophthalmol.* 2018;96:e911–e918.
4. Vujosevic S, Vaclavik V, Bird AC, Leung I, Dandekar S, Peto T. Combined grading for choroidal neovascularisation: colour, fluorescein angiography and autofluorescence images. *Graefes Arch Clin Exp Ophthalmol.* 2007;245:1453–1460.
5. Vaclavik V, Vujosevic S, Dandekar SS, Bunce C, Peto T, Bird AC. Autofluorescence imaging in age-related macular degeneration complicated by neovascularization: a prospective study. *Ophthalmology.* 2008;115:342–346.
6. McBain VA, Townend J, Lois N. Fundus autofluorescence in exudative age-related macular degeneration. *Br J Ophthalmol.* 2007;91:491–496.
7. Schmitz-Valckenberg S, Holz FG, Bird AC, Spaide RF. Fundus autofluorescence imaging: review and perspectives. *Retina.* 2008;28:385–409.
8. McLeod DS, Grebe R, Bhutto I, Merges C, Baba T, Lutty GA. Relationship between RPE and chirocapillaris in age-related macular degeneration. *Invest Ophthalmol Vis Sci.* 2009;50:4982–4991.
9. Gabai A, Veritti D, Lanzetta P. Fundus autofluorescence applications in retinal imaging. *Indian J Ophthalmol.* 2015;63:406–415.
10. Delori FC, Dorey CK, Staurenghi G, Arend O, Goger DG, Weiter JJ. In vivo fluorescence of the ocular fundus exhibits retinal pigment epithelium lipofuscin characteristics. *Invest Ophthalmol Vis Sci.* 1995;36:718–729.
11. Croce AC, Bottiroli G. Autofluorescence spectroscopy and imaging: a tool for biomedical research and diagnosis. *Eur J Histochem.* 2014;58:2461.
12. Hammer M, Königsdörffer E, Liebermann C, et al. Ocular fundus auto-fluorescence observations at different wavelengths in patients with age-related macular degenerazion and diabetic retinopathy. *Graefes Arch Clin Exp Ophthalmol.* 2008;246:979–988.
13. Munch G, Thome J, Foley P, Schinzel R, Riederer P. Advanced glycation endproducts in ageing and Alzheimer's disease. *Brain Res Brain Res Rev.* 1997;23:134–143.
14. Borrelli E, Lei J, Balasubramanian S, et al. Green emission fluorophores in eyes with atrophic age-related macular degeneration: a colour fundus autofluorescence pilot study. *Br J Ophthalmol.* 2018;102:827–832.
15. Borrelli E, Nittala MG, Abdelfattah NS, et al. Comparison of short-wavelength blue-light autofluorescence and conventional blue-light autofluorescence in geographic atrophy. *Br J Ophthalmol.* 2018;103(5):610–616.
16. Ravera V, Giani A, Pellegrini M, et al. Comparison among different diagnostic methods in the study of type and activity of choroidal neovascular membranes in age-related macular degeneration. *Retina*. 2019;39:281–287.
17. Khurana RN, Hill L, Ghanekar A, Gune S. Agreement of spectral domain optical coherence tomography with fluorescein leakage in neovascular age-related macular degeneration: post hoc

analysis of the HARBOR study. *Ophthalmol Retina.* 2020;4(11):1054–1058.
18. Vujosevic S, Toma C, Nucci P, et al. Quantitative color fundus autofluorescence in patients with diabetes mellitus. *J Clin Med*. 2020;10:E48.
19. Chaudhuri J, Bains Y, Guha S, et al. The role of advanced glycation end products in aging and metabolic diseases: bridging association and causality. *Cell Metab.* 2018;28:337–352.
20. Ishibashi T, Murata T, Hangai M, et al. Advanced glycation end products in age-related macular degeneration. *Arch Ophthalmol.* 1998;116:1629–1632.
21. Schweitzer D, Schenke S, Hammer M, et al. Towards metabolic mapping of the human retina. *Microsc Res Tech.* 2007;70:410–419.
22. Marmorstein AD, Marmorstein LY, Sakaguchi H, Hollyfield JG. Spectral profiling of autofluorescence associated with lipofuscin, Bruch's membrane, and sub-RPE deposits in normal and AMD eyes. *Invest Ophthalmol Vis Sci.* 2002;43:2435–2441.
23. Fleckenstein M, Charbel Issa P, Helb HM, et al. High-resolution spectral domain-OCT imaging in geographic atrophy associated with age-related macular degeneration. *Invest Ophthalmol Vis Sci.* 2008;49:4137.
24. Borrelli E, Battista M, Zuccaro B, et al. Spectrally resolved fundus autofluorescence in healthy eyes: repeatability and topographical analysis of the green-emitting fluorophores. *J Clin Med*. 2020;9:2388.
25. Curcio CA. Soft drusen in age-related macular degeneration: biology and targeting, via the Oil Spill strategies. *Invest Ophthalmol Vis Sci.* 2018;59:AMD160–AMD181.
26. Lu M, Kuroki M, Amano S, et al. Advanced glycation end products increase retinal vascular endothelial growth factor expression. *J Clin Invest.* 1998;101:1219–1224.
27. Yamagishi S, Yonekura H, Yamamoto Y, et al. Advanced glycation end products-driven angiogenesis in vitro: induction of the growth and tube formation of human microvascular endothelial cells through autocrine vascular endothelial growth factor. *J Biol Chem.* 1997;272:8723–8730.
28. Makino H, Shikata K, Kushiro M, et al. Roles of advanced glycation end-products in the progression of diabetic nephropathy. *Nephrol Dial Transplant.* 1996;11:76–80.
29. Handa JT, Reiser KM, Matsunaga H, Hjelmeland LM. The advanced glycation endproduct pentosidine induces the expression of PDGF-B in human retinal pigment epithelial cells. *Exp Eye Res.* 1998;66:411–419.
30. Parekh PK, Folk JC, Gupta P, Russell SR, Sohn EH, Abràmoff MD. Fluorescein angiography does not alter the initial clinical management of choroidal neovascularization in age-related macular degeneration. *Ophthalmol Retina.* 2018;2:659–666.
31. Jaffe GJ, Martin DF, Toth CA, et al. Macular morphology and visual acuity in the comparison of age-related macular degeneration treatments trials. *Ophthalmology.* 2013;120:1860–1870.
32. Karadimas P, Bouzas EA. Fundus autofluorescence imaging in serous and drusenoid pigment epithelial detachments associated with age-related macular degeneration. *Am J Ophthalmol.* 2005;140:1163–1165.
33. Lois N, Owens SL, Coco R, Hopkins J, Fitzke FW, Bird AC. Fundus autofluorescence in patients with age-related macular degeneration and high risk of visual loss. *Am J Ophthalmol.* 2002;133:341–349.
34. Spital G, Radermacher M, Muller C, Brumm G, Lommatzsch A, Pauleikhoff D. Autofluorescence characteristics of lipofuscin components in different forms of late senile macular degeneration. *Klin Monatsbl Augenheilkd*. 1998;213:23–31.
35. Spaide RF. Fundus autofluorescence and age-related macular degeneration. *Ophthalmology*. 2003;110:392–399.
36. Von Ruckmann A, Fitzke FW, Bird AC. Fundus autofluorescence in age-related macular disease imaged with a laser scanning ophthalmoscope. *Invest Ophthalmol Vis Sci.* 1997;38:478–486.
37. Ivert L, Kjeldbye H, Gouras P. Long-term effects of short-term retinal bleb detachments in rabbits. *Graefes Arch Clin Exp Ophthalmol.* 2002;240:232–237.
38. Framme C, Walter A, Gabler B, Roider J, Sachs HG, Gabel VP. Fundus autofluorescence in acute and chronic-recurrent central serous chorioretinopathy. *Acta Ophthalmol Scand.* 2005;83:161–167.